

SHORT  
COMMUNICATIONS

## Rare Earth Elements in the Ores of Epithermal Gold–Silver and Silver Deposits, Russia's Northeast

R. G. Kravtsova and Ya. A. Almaz

*Vinogradov Institute of Geochemistry, Siberian Division, Russian Academy of Sciences,  
ul. Favorskogo 1a, Irkutsk, 664033 Russia*

*e-mail: krg@igc.irk.ru*

Received May 16, 2005

DOI: 10.1134/S001670290612007X

Relations between mineralization and magmatic rocks and sources of ore-forming fluids are presently among the most important problems in endogenous ore formation. Geochemical methods provide a valuable insight into these problems. The estimation of ore potential and search for reliable criteria for the determination of sources of ore elements are based mainly on the study and comparison of the ore-element compositions of rocks and ores. In this study, we attempted to solve these problems by a nontraditional way, studying REE distribution in ores and comparing it with the behavior of these elements in igneous rocks.

The distribution of REEs in ores was studied by the example of epithermal deposits and occurrences of gold–silver (Au–Ag), silver–base metal (Ag–Pb), and tin–silver (Sn–Ag) associations. All the objects are located within the largest ore-bearing structures in the central part of the Okhotsk–Chukchi volcanic belt (OCVB): the Turomchin (Dal'nee and Kwartsevaya Sopka Au–Ag deposits and Al'dygich occurrence) and Arman (Katamken Au–Ag deposit) ring volcanic structures and the Dukat volcanoplutonic uplift (Dukat Au–Ag deposit, Mechta and Tidit Ag–Pb deposits, Maliy Ken Sn–Ag deposit, and Final'noe occurrence). The geology, mineralogy, and geochemistry of the deposits and occurrences were reported in [1–10 etc.]. However, there is no information on REE distribution in epithermal Au–Ag, Ag–Pb, and Sn–Ag ores, both in the Russian and international literature. This is the first such investigation.

Rare-earth elements were analyzed by spectroscopic methods [11]. Analysts were E.V. Smirnova and T.N. Galkina. To compare LREEs and HREEs, the  $\Sigma$ REE and the proportions of REE groups  $\Sigma_{Ce}$ ,  $\Sigma_{Y}$ ,  $\Sigma_{Sc}$  were calculated [12]. The Eu/Sm ratio was used to estimate the depth of formation of ores using the interpretation of [13]. The redox conditions of ore-forming environments were estimated using the Eu/Ce ratio, and the degree of LREE and HREE differentiation was characterized by the Ce/Yb ratio. The distribution of REEs in the rocks of the ore-bearing structures and

deposits were previously investigated in [14–17]. All these data were generalized and are considered below.

The magmatic rocks of the ore-bearing structures are mainly represented by the subduction-related calc-alkaline andesite and postsubduction subalkaline trachyrhyolite–basalt associations of the OCVB [4, 5, 16, 17].

The magmatic rocks of the later contrasting bimodal trachyrhyolite–basaltic series are widespread only at the Dukat Uplift, where they form an independent rhyodacite–leucogranite association enriched in Ag, Sn, and base metals [5, 17]. The wall rocks are silicic volcanics. The leucogranites and rhyodacites show  $\Sigma$ PREE values of 288 and 157–203 ppm, respectively. Their REE proportions are nearly identical:  $77_{Ce}16_{Y}7_{Sc}$  and  $78_{Ce}16_{Y}6_{Sc}$ , respectively. The degree of LREE enrichment increases slightly. The average Ce/Yb ratios are 11 and 14, respectively. The similar Eu/Sm (0.1–0.2) and Eu/Ce (0.003–0.007) ratios in the rocks of the rhyodacite–leucogranite association testify to similar conditions of their formation. Figures 1 and 2 present REE distribution patterns for the leucogranites of the Dukat Massif (average of 11 samples), which reflect the main characteristic features of this association.

Rocks of the calc-alkaline andesite association are most abundant in the ore-bearing structures studied (Turomchin, Arman, and Dukat). An andesite–granodiorite volcanoplutonic association was distinguished there. It is closely related in space and time with typical epithermal Au–Ag ores of volcanogenic deposits [3, 4, 5, 8]. The REEs were analyzed mainly in andesite series rocks: andesites, basaltic andesites, dacite porphyrites, and diorites. The host rocks are intermediate volcanics. The lowest  $\Sigma$ REE (70.5–107 ppm) were found in unaltered andesites from all the ore-bearing structures, and the highest  $\Sigma$ REE values are confined to the weakly altered andesites (162 ppm) of the Turomchin volcanic structure and diorite porphyrites (154 ppm) of the Dukat Uplift. The rocks of the andesite series display similar REE patterns with low REE totals and a weak negative Eu anomaly [14], which are strongly different from those of the rhyodacite–leucogranite association [15]. There

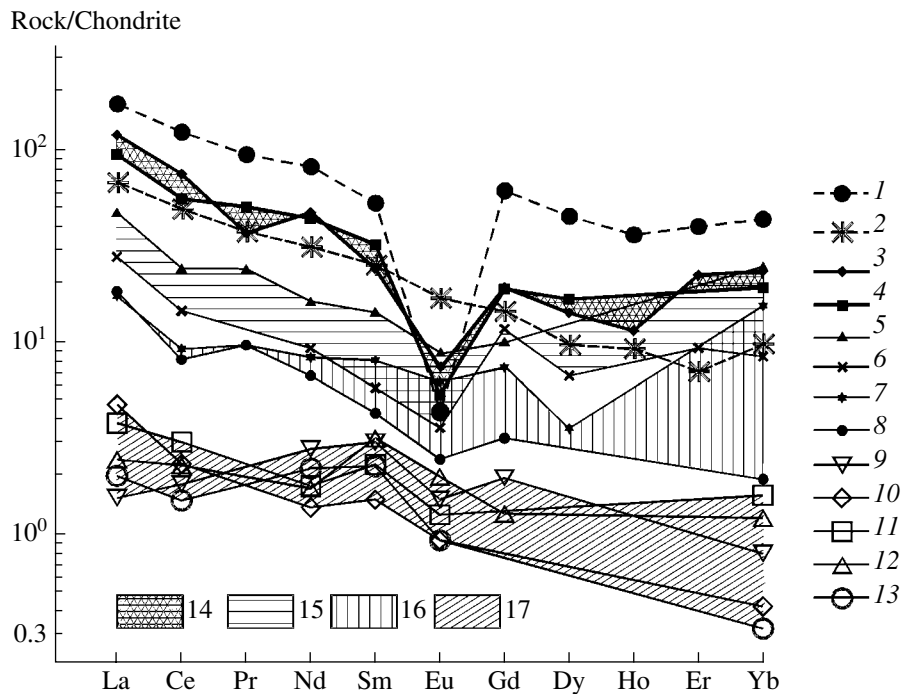


**Fig. 1.** REE contents in the rocks of the central part of the OCVB and ores of the Dukat ore cluster. Rocks: (1) final-stage leucogranite of the Dukat Massif (average of 11 samples), (2) continental-margin andesite (average of 15 samples). Ores: (14) Sn–Ag (3, 4); (15) Sn–Ag–Pb (5, 6); (16) Ag–Pb (7, 8); (17) Au–Ag (9–11), and Ag (12, 13). Symbols correspond to numbers in Table 1. Here and in Fig. 2, REE contents are normalized to chondrite values [18].

is LREE enrichment, especially pronounced in the andesites:  $81_{\text{Ce}}13_{\text{Y}}6_{\text{Sc}}-84_{\text{Ce}}14_{\text{Y}}2_{\text{Sc}}$ . The REE distribution patterns of andesites and diorites are sharply different from those of leucogranites. Their REE abundances are two to four times lower, except for Eu, which is three to five times higher relative to the silicic rocks. The low REE totals (70.5 ppm or lower), high Eu/Sm ratios ( $>0.6$ ), and the absence of a Eu anomaly indicate that the rocks of the andesite series could be derivatives of basaltic melts [14, 16]. In the chondrite-normalized diagrams (Figs. 1, 2), these rocks are represented by continental-margin andesites of the calc-alkaline series (average of 15 samples).

The contents and distribution of REEs in the ores of the Au–Ag, Ag–Pb, and Sn–Ag deposits and occurrences of the Dukat volcanoplutonic uplift were defined by the evolution of the rhyodacite–leucogranite rock association. Unlike the ores of the Turmchin and Arkan deposits, these ores underwent a longer and more complex evolution. The beginning of hydrothermal activity produced Sn–Ag and then Ag–Pb mineralization. The Sn–Ag ores are ascribed to the stringer-disseminated type. The stringers are quartz–sulfide and chlorite–biotite–sulfide in composition (Malyi Koen). The main ore minerals are argentite, stannite, cassiterite, chalcocopyrite, sphalerite, galena, pyrite, arsenopyrite, and, occasionally, fahlores and tourmaline. The Ag–Pb mineralization occurs as vein-type ores (Mechta and Tidit). The veins have sulfide–quartz and sulfide–

carbonate–quartz compositions. Hydromica, apatite, and epidote occur in subordinate amounts. The most abundant ore minerals are galena, sphalerite, arsenopyrite, chalcocopyrite, and freibergite. Pyrite, marcasite, boulangerite, stannite, pyrargyrite, and stephanite are less common. Miargyrite, diaphthorite, acanthite, polybasite, alargentum, and native silver occur in very minor amounts [1, 7, 10].

The later Au–Ag and Ag ores of the Dukat deposit are characterized by polychronous evolution and complex mineral and component compositions [2, 5, 6, 9, etc.]. The ores of the deposit provide a typical example of rejuvenated pregranite Au–Ag mineralization. The rejuvenation was promoted by the emplacement of a rare-metal granitoid intrusion (Dukat Massif). Based on mineralogy, ore geochemistry, and spatial variations, three main productive stages can be distinguished (in order of their formation): Ag–Pb, Au–Ag, and late Ag-dominated. The footwall levels bear distinct polysulfide (Sn–Ag–Pb) noncommercial mineralization. The Ag-dominated ores are composed mainly of native silver, kustelite, and Ag sulfoantimonides. The Au–Ag ores are made up of acanthite and Ag sulfoarsenide. The Ag–Pb and Sn–Ag–Pb ores are composed of galena, sphalerite, freibergite, and stannite. There are also rare-metal minerals, such as helvite, spessartite, and axinite.

All the ores are characterized by relatively low REE contents as compared to their host rocks (Table 1). Low

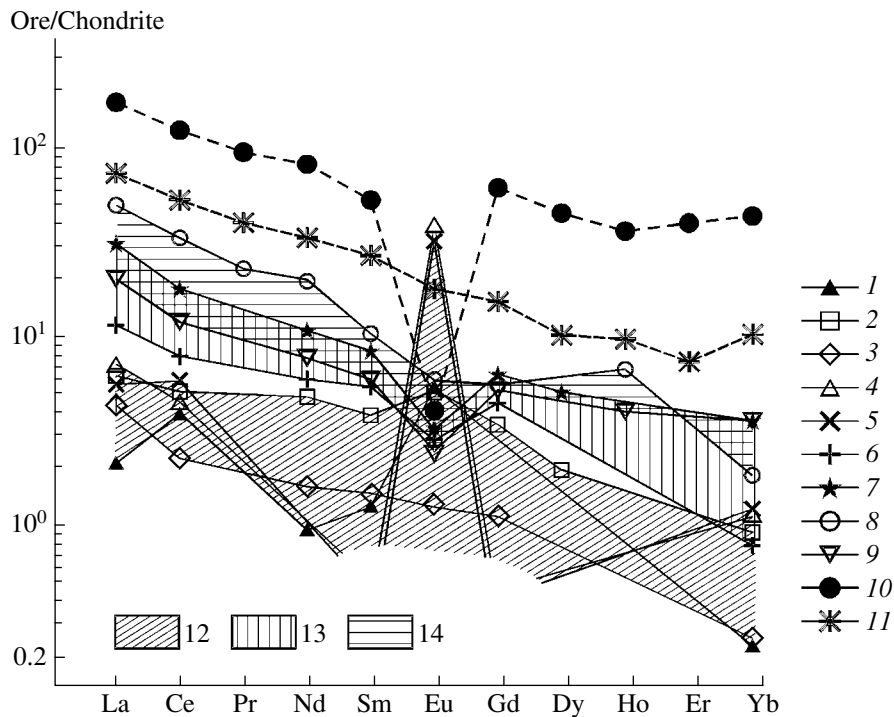


**Fig. 2.** REE contents in the rocks of the central part of the OVCB and in the ores from the deposits and occurrences of the Turomchin and Arman volcanic structures. Rocks: (10) final-stage leucogarnite of the Dukat Massif (average of 11 samples) and (11) continental-margin andesite (average of 15 samples). Ores: (12) Au–Ag (1–5), (13) Au–Ag sulfide (6, 7), (14) Ag sulfide–Ag–Pb–Zn (8, 9). Numbers (1–9) correspond to numbers in Table 2, and (10 and 11) correspond to numbers 1 and 2, respectively, in Table 1.

total REE concentrations (up to 5.7 ppm) were found in the ore bodies at the upper–middle ore levels of the central part of the Dukat deposit, where abundant rejuvenated Au–Ag and Ag ores occur in quartz–feldspar–rhodonite and quartz–rhodonite veins. Low total REE contents (up to 28 ppm) were detected in the quartz–base metal veins of Ag–Pb ores (Mechta, Tidit, and lower–middle ore levels of the Dukat deposit). Elevated (up to 60 ppm) and high (up to 160 ppm) REE contents were found only in the quartz–chlorite–polysulfide veins bearing Sn–Ag mineralization (Malyi Koen and Final’noe) and in the quartz–chlorite–base metal veins of the lower ore levels of the Dukat deposit with Sn–Ag–Pb mineralization.

Similar to all other complexes considered above, the REE distribution patterns of the ores are enriched to the highest degree in Ce-group REEs. The average REE proportions are as follows:  $81_{Ce}13_{Y}6_{Sc}$  in the Sn–Ag and Sn–Ag–Pb ores,  $80_{Ce}14_{Y}6_{Sc}$  in the Ag–Pb ores, and  $81_{Ce}15_{Y}4_{Sc}$  in the Au–Ag and Ag ores. The proportions of Ce-group REEs in most rocks are similar to those of the leucogranite series. This is most distinctly seen from the low Ce/Yb ratios. This ratio averages 11 both in the ores and in the leucogranites. The Eu/Ce ratio increases regularly from 0.009 to 0.083. The same is true for the Eu/Sm ratio varying within 0.39–0.91 in the Sn–Ag ores and 0.40–0.66 in the Au–Ag and Ag ores. The low Eu/Sm ratios (<1) in the unaltered rocks and ores indicate that all pre-ore and ore processes related

to the emplacement of a granitoid intrusion took place in the upper crust under relatively oxidizing conditions at similar depths [13].

The character of REE behavior during hydrothermal ore formation and changes in their distribution at different stages are clearly expressed in the REE patterns shown in Fig. 1. Each ore type has its distinctive REE pattern. The early Sn–Ag ores show the highest REE contents and a distinct negative Eu anomaly. Their patterns are most similar to those of the rhyodacite–leucogranite series. The later Au–Ag ores show a regular decrease in REE contents and the magnitude of Eu anomaly. The lowest REE contents were observed in the latest Au–Ag and Ag ores. These ores show a weak negative or no Eu anomaly. The REE distribution patterns of the rejuvenated Au–Ag and Ag ores are similar to those of the andesite series. In our opinion, this fact confirms the mixed mantle–crustal origin of the ores [2, 5].

The epithermal Au–Ag ores formed within the Turomchin and Arman volcanic structures reveal even a closer relation with mantle fluids [5, 16]. All ores of typical volcanogenic Au–Ag deposits, including those studied here, have two-metal low-sulfide compositions. Only two elements, Au and Ag, occur in commercial concentrations. The gangue minerals are quartz, adularia, sericite, hydromica, and, occasionally, carbonate and kaolinite. Ore minerals account for no more than 1–3%. The main ore minerals are argentite, electrum, proustite, pyrrargyrite, native gold and silver, polybasite, and

**Table 1.** Concentrations of REEs (ppm) in the rocks of the central part of the OCVB and in the ores of the deposits of the Dukat ore cluster

Component	1	2	3	4	5	6	7	8	9	10	11	12	13
La	56	23	38	30	15	8.8	5.5	5.8	0.8	1.5	1.2	0.9	0.7
Ce	104	43	62	46	20	12	7.6	7.1	1.5	2.0	2.5	1.8	1.4
Pr	12	4.9	4.6	6.3	3.0	<1	1.2	1.2	<1	<1	<1	<1	<1
Nd	51	20	29	27	10	5.7	5.1	4.1	1.7	1.0	1.1	1.0	1.2
Sm	10.7	5.2	4.8	6.4	2.8	1.2	1.6	0.9	0.6	0.4	0.5	0.6	0.5
Eu	0.33	1.3	0.70	0.40	0.87	0.27	0.55	0.17	0.09	0.07	0.08	0.15	0.07
Gd	16.5	3.9	5.1	5.0	2.6	2.6	2.0	0.8	0.5	<0.3	<0.3	0.3	<0.3
Dy	15.1	3.2	5.0	5.5	<0.7	2.2	0.8	<0.7	<0.7	<0.7	<0.7	<0.7	<0.7
Ho	2.7	0.68	0.8	<0.5	<0.5	<0.5	<0.5	<0.5	<0.5	<0.5	<0.5	<0.5	<0.5
Er	8.7	1.5	4.8	<1	<1	2.0	<1	<1	<1	<1	<1	<1	<1
Yb	9.4	2.1	5.0	4.1	5.3	1.8	3.3	0.33	0.17	0.09	0.34	0.30	0.07
ΣREE	288*	109*	160	131	60	37	28	20	5.4	5.1	5.7	5.1	3.9
Eu/Sm( <i>n</i> )	0.08	0.66	0.39	0.17	0.82	0.60	0.91	0.50	0.40	0.46	0.42	0.66	0.37
Eu/Ce	0.003	0.030	0.011	0.009	0.044	0.023	0.072	0.024	0.060	0.035	0.032	0.083	0.050
Ce/Yb	11	21	12	11	4	7	2	22	9	22	7	6	20
ΣCe, %	77	83	84	84	81	73	70	89	75	89	84	73	84
ΣY, %	16	13	10	13	10	17	17	9	22	9	10	21	14
ΣSc, %	7	4	6	3	9	10	13	2	3	2	6	6	2

Note: (1) Final-stage leucogranite of the Dukat Massif (average of 11 samples); (2) continental-margin andesite (average of 15 samples); (3, 4) Sn–Ag ores: (3) quartz–chlorite–polysulfide veins, Malyi Ken deposit, and (4) Final'noe occurrence; (5, 6) Sn–Ag–Pb ores: (5) quartz–chlorite–base-metal veins, Malyi Ken deposit and (6) lower level of the Dukat deposit; (7, 8) Ag–Pb ores: quartz–base-metal veins, (7) Mehta and (8) Tidit deposits; (9–11) Au–Ag ores: (9, 10) quartz–feldspar–rhodonite veins, Dukat deposit, and (11) Smelyi area, flank of the Dukat deposit; (12, 13) Ag ores: (12) quartz–rhodonite and (13) pyrolusite–quartz veins, Dukat deposit.

\* Here and in further calculations, ΣREE includes 1.52 ppm Lu in leucogranites and 0.3 ppm Lu in andesites.

stromeyerite. Less common minerals are galena, sphalerite, chalcopyrite, arsenopyrite, miargyrite, pearceite, and stephanite; native As, fahlores, stibnite, hessite, petzite, freibergite, and canfieldite were observed in rare cases [3, 4, 8].

Table 2 presents the concentrations and distribution of REEs in these rocks. Low REE contents (5.6–12.2 ppm) were found in the high-grade Au–Ag quartz–adularia veins at the upper–middle levels of Au–Ag deposits (Dal'nee and Karamken). Rather low REE contents (16.7–37.8 ppm) were determined in the low-grade quartz–adularia–sulfide veins (Au–Ag sulfide ores) at the lower ore horizons of Au–Ag deposits (Dal'nee and Kwartsevaya Sopka). Elevated REE contents (25.2–64.7 ppm) were found only in the zones of Ag–sulfide (Ag–Pb–Zn ores) mineralization at the flanks of ore fields (Al'dylich) and deposits (Karamken). The mineralization is represented by stringer–disseminated ores among pervasively altered andesites. The REE distribution patterns of the Ag–Pb–Zn ores show even greater LREE enrichment than the previously considered complexes. The average proportions of REE groups are  $88_{\text{Ce}}10_{\text{Y}}2_{\text{Sc}}$  in the Ag–sulfide ores,  $84_{\text{Ce}}14_{\text{Y}}2_{\text{Sc}}$  in the Au–Ag sulfide ores, and  $81_{\text{Ce}}17_{\text{Y}}2_{\text{Sc}}$  in the Au–Ag ores.

These characteristics are similar to those of andesites. The ores are severely depleted in HREEs. This is most clearly seen from Ce/Yb ratios, which are strongly different in the ores of the Turomchin and Arman volcanic structures and those related to the Dukat volcanoplutonic uplift. This ratio averages 45 in the Au–Ag volcanogenic ores and 50 in the Ag–Pb–Zn ores and is similar to that of andesites (21). The Eu/Ce ratio increases significantly (0.053–0.792). The same trend is observed for the Eu/Sm ratio varying within 0.88–3.10 in the Au–Ag ores. These values are significantly higher than those observed at the Dukat deposits and comparable with the Eu/Sm ratios of the andesite series (0.66). These observations confirm the greater depths of formation of Au–Ag volcanogenic ores as compared to subsurface rejuvenated Au–Ag ores formed in the volcanoplutonic uplift.

Ore varieties typical of volcanic structures can be also distinctly distinguished by their REE distribution patterns (Fig. 2). The highest REE contents and a pronounced negative Eu anomaly were detected in the Ag–Pb–Zn ores (flanks of ore fields and deposits). These values are slightly lower in the Au–Ag sulfide ores (low ore levels of Au–Ag deposits) and reach min-

**Table 2.** Concentrations of REEs (ppm) in the ores of the deposits and occurrences of the Turomchin and Arman volcanic structures

Component	1	2	3	4	5	6	7	8	9
La	0.69	2.01	1.40	2.30	1.80	3.70	10.01	16.02	6.50
Ce	3.6	4.3	1.9	3.8	4.5	6.6	15.0	28.0	10.0
Pr	<1.0	<1.0	<1.0	<1.0	<1.0	<1.0	<1.0	2.9	<1.0
Nd	0.6	3.0	1.0	<0.3	<0.3	3.7	6.7	13.0	4.8
Sm	0.3	0.8	0.3	<0.3	<0.3	1.1	1.7	2.1	1.2
Eu	0.35	0.33	0.10	3.01	2.80	0.20	0.23	0.40	0.20
Gd	<0.3	0.9	0.3	<0.3	<0.3	1.2	1.7	1.5	1.4
Dy	<0.7	0.7	<0.7	<0.7	<0.7	<0.7	1.7	<0.7	<0.7
Ho	<0.5	<0.5	<0.5	<0.5	<0.5	<0.5	<0.5	0.5	0.5
Er	<1.0	<1.0	<1.0	<1.0	<1.0	<1.0	<1.0	<1.0	<1.0
Yb	0.05	0.20	0.05	0.26	0.26	0.17	0.78	0.32	0.78
ΣREE	5.6	12.2	5.1	9.37	9.36	16.7	37.8	64.7	25.38
Eu/Sm( <i>n</i> )	3.10	1.09	0.88	–	–	0.48	0.36	0.51	0.44
Eu/Ce	0.097	0.077	0.053	0.792	0.622	0.030	0.015	0.014	0.020
Ce/Yb	72	22	38	15	17	39	19	88	13
ΣCe, %	87	76	85	65	67	84	84	93	84
ΣY, %	12	22	14	32	30	15	14	7	13
ΣSc, %	1	2	1	3	3	1	2	0	3

Note: (1, 2, 3) Au–Ag ores, Dal'nee deposit: (1) quartz–adularia vein with clasts of strongly altered host rocks, upper–middle ore level; (2) quartz–adularia vein with poor sulfide mineralization, upper–middle ore level; and (3) quartz–adularia vein, lower ore level; (4, 5) Au–Ag ores, Karamken deposits, quartz–adularia veins with poor sulfide mineralization, upper ore levels; (6, 7) Au–Ag sulfide ores, quartz–adularia–sulfide veins, lower ore levels, (6) Dal'nee and (7) Kvarsevaya Sopka deposits; (8, 9) Ag–sulfide (Au–Pb–Zn) mineralization with low Au content (tenths of ppm): (8) zone of stringer–disseminated sulfide (galena, sphalerite, chalcopyrite) mineralization in strongly altered pyritized andesites, Al'dylich occurrence, southeastern flank of the Turomchin volcanic structure; and (9) ore metasomatite, andesite completely replaced by quartz, hydromica, and pyrite with large amounts of quartz–base-metal stringers, northern flank of the Karamken deposit, Arman volcanic structure.

imum levels at the upper–middle zones of Au–Ag deposits. Most of the Au–Ag ores show high Eu contents (up to 3 ppm), which are expressed as positive anomalies in the REE distribution patterns. The REE distribution patterns of the Au–Ag ores are even more similar than those of the Dukat deposit to the REE patterns of andesite series, which are derivatives of mantle basaltoid magmas [15, 16]. The data obtained in this study suggest that andesite magmas are the most probable source of fluids that were responsible for the formation of typical Au–Ag ores and supplied Au and Ag into all later types of Au–Ag ores.

Our investigations showed that the distribution of REEs in ores is an efficient tool to study epithermal deposits of the Au–Ag, Ag–Pb, and Sn–Ag associations. It was established for the first time that REEs are sensitive indicators of the ore source, sequence of processes, and physicochemical conditions. The Eu/Sm ratio is indicative of both the depth of formation of ore-forming fluid systems at different (lower and upper) crustal levels [13] and the relative depths of formation of different ores within local intervals. It was shown for the first time that each ore type is characterized by spe-

cific REE contents and distribution patterns, which can be used as an efficient geochemical tool in assigning the revealed mineralization to a particular ore association. The distribution of REEs is distinctly zoned. As fluids are formed and ascent during ore formation, the total REE content tends to decrease concurrently with an increase in the relative fraction of LREEs.

#### ACKNOWLEDGMENTS

The study was financially supported by the Russian Foundation for Basic Research (project no. 04-05-64201) and the Siberian Division of the Russian Academy of Sciences (project no. 71).

#### REFERENCES

1. M. M. Konstantinov, A. V. Kostin, and A. A. Sidorov, *Geology of Silver Deposits*, (Yakutsk, 2003) [in Russian].
2. M. M. Konstantinov, V. E. Natalenko, A. I. Kalinin, and S. F. Struzhkov, *The Dukat Gold–Silver Deposit* (Nedra, Moscow, 1998) [in Russian].

3. N. A. Kostyrko, L. N. Plyashkevich, and M. V. Boldyrev, "Structure and Composition of Ore Zones in the Evensk Ore Field," in *Proceedings on the Geology and Mineral Resources of Russian Northeast* (Magadan, 1974) **21**, pp. 87–94 [in Russian].
4. R. G. Kravtsova, "Mineralogical and Geochemical Zoning and Genesis of Gold–Silver Deposits, Russia's Northeast," *Geol. Geofiz.* **39**, 763–777 (1998).
5. R. G. Kravtsova, A. A. Borovikov, A. S. Borisenko, and V. Yu. Prokof'ev, "Formation Conditions of Gold–Silver Deposits in the Northern Okhotsk Region, Russia," *Geol. Rudn. Mestorozhd.* **45**, 452–473 (2003) [*Geol. Ore Dep.* **45**, 395–415 (2003)].
6. R. G. Kravtsova and M. N. Zakharov, "Geochemical Accumulation Fields of the Dukat Gold–Silver Ore–Magmatic System, Northeastern Russia," *Geol. Geofiz.* **37** (5), 28–38 (1996).
7. R. G. Kravtsova, M. N. Zakharov, and N. G. Shatkov, "Mineralogical and Geochemical Features of Host Rocks of the Gol'tsovoe Silver–Base Metal Deposit (Northeastern Russia)," *Geol. Rudn. Mestorozhd.* **40**, 221–235 (1998) [*Geol. Ore Dep.* **40**, 197–210 (1998)].
8. A. N. Nekrasova, A. A. Krasil'nikov, and G. P. Demin, "Endogenous Ore Zoning in the Volcanogenic Gold–Silver Deposits," *Sov. Geol.*, No. 1, 105–110 (1979).
9. I. S. Raevskaya and A. I. Kalinin, "Mineral Features and Zoning of a Gold–Silver Deposit in the Okhotsk–Chukchi Volcanogenic Belt," in *Mineral Types of Ore Deposits in the Volcanic Belts and Activation Zones of Northeastern Asia* (Vladivostok, 1983), pp. 41–50 [in Russian].
10. Yu. N. Rodnov and V. I. Zaitsev, "Relations between Tin and Silver Mineralization in the Balygychan–Sugoisk Area, Russia's Northeast," in *Magmatism of the Ore Districts of Russia's Far East* (DVNTS Akad. Nauk SSSR, Vladivostok, 1985), pp. 155–167 [in Russian].
11. E. V. Smirnova, A. I. Kuznetsova, and N. L. Chumakova, *Atomic-Emission Analysis in Geochemistry* (Nauka, Novosibirsk, 1993) [in Russian].
12. D. A. Mineev, *Lanthanides in the Ores of Rare-Earth and Combined Deposits* (Nauka, Moscow, 1974) [in Russian].
13. S. F. Vinokurov, "Europium Anomalies in Ore Deposits and Their Geochemical Significance," *Dokl. Akad. Nauk* **346**, 792–795 (1996) [*Dokl. Earth Sci.* **347**, 281–283 (1996)].
14. M. N. Zakharov, V. V. Konusova, and E. V. Smirnova, "Rare-Earth Elements in the Basalts of the Omolon Area, Okhotsk–Chukchi Volcanogenic Belt," *Geol. Geofiz.*, No. 4, 62–70 (1984).
15. M. N. Zakharov, V. V. Konusova, and E. V. Smirnova, "Rare-Earth Element Distribution in the Felsic Rocks of Volcanoplutonic Associations, Okhotsk Segment of the Okhotsk–Chukchi Volcanogenic Belt," *Geokhimiya*, No. 12, 1796–1805 (1990).
16. M. N. Zakharov and R. G. Kravtsova, "Geochemistry of Rocks from Volcanic–Plutonic Associations at the Karamken Gold–Silver Deposit, Russian Northeast," *Geokhimiya*, No. 9, 933–942 (2001) [*Geochem. Int.* **39**, 848–856 (2001)].
17. M. N. Zakharov, R. G. Kravtsova, and L. A. Pavlova, "Geochemical Features of Rocks from the Volcanoplutonic Associations of the Dukat Gold–Silver Deposit," *Geol. Geofiz.* **43**, 928–939 (2002).
18. W. V. Boynton, "Cosmochemistry of the Rare Earth Elements. Meteorite Studies," in *Rare Earth Elements Geochemistry* (Elsevier, Amsterdam, 1984), Vol. 2, pp. 63–114.